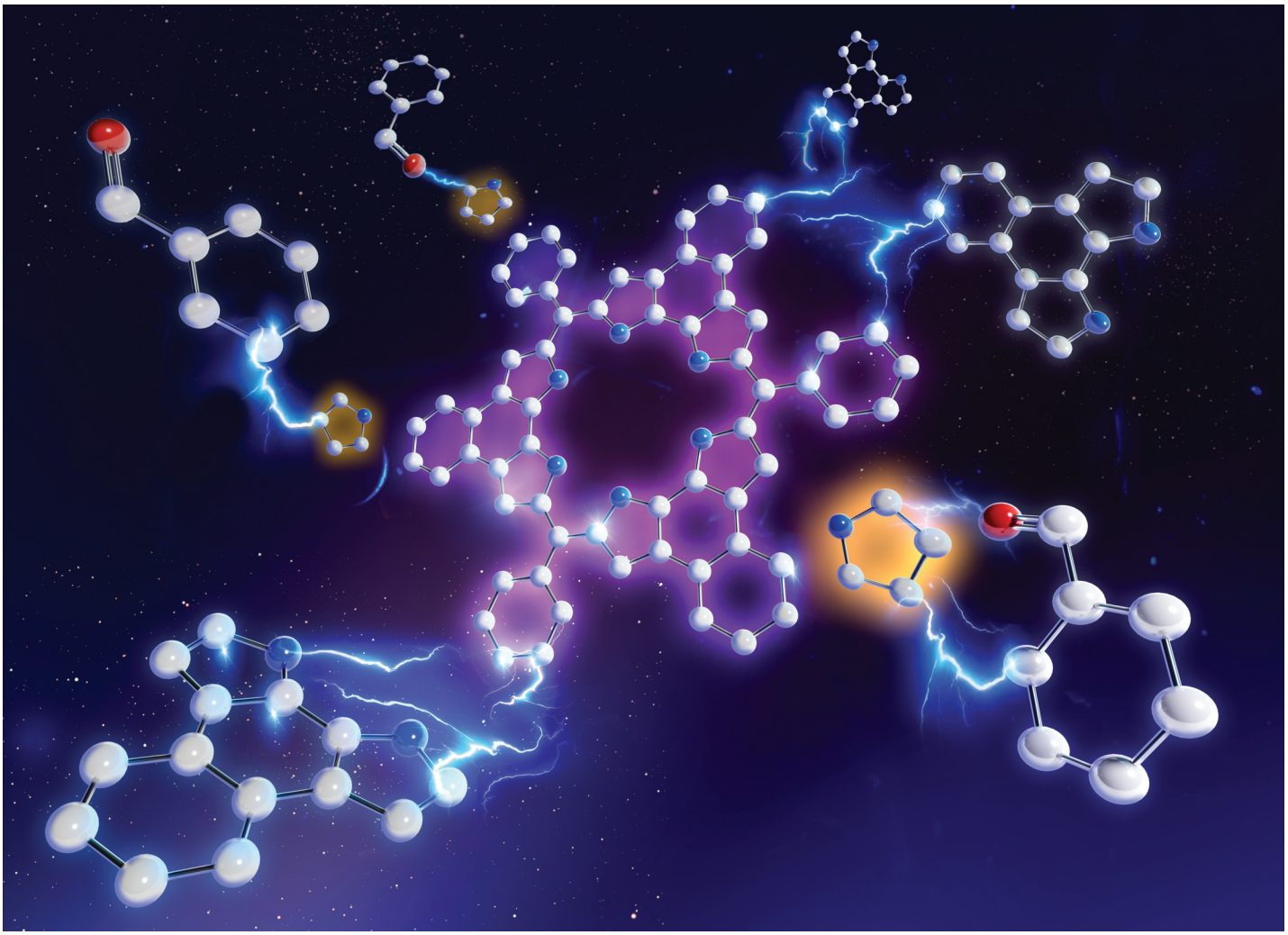

Showcasing research from Professor Torres's laboratory, Department of Organic Chemistry, Autonomous University of Madrid, Madrid, Spain and Professor Sessler's laboratory, Department of Chemistry, The University of Texas at Austin, Austin, Texas, USA.

Synthesis of annulated rosarins *via* iminium activation

This research presents a novel approach to the complex construction of pyrrolic macrocycles using activated aldehydes, facilitated by pre-conversion into corresponding iminium species. The newly synthesized macrocycles demonstrate that this method outperforms classical methodologies. Theoretical calculations provide support for the conclusion that iminium pathways make condensation reactions both kinetically and thermodynamically more favourable, paving the way for the synthesis of previously inaccessible systems.

Image created by Nhat Nam Vu.

As featured in:

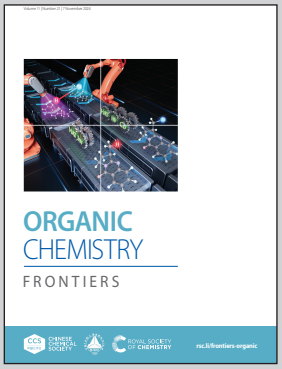

See Jorge Labella, Tomás Torres, Jonathan L. Sessler *et al.*, *Org. Chem. Front.*, 2024, **11**, 6036.

CCS 中国化学会 CHINESE CHEMICAL SOCIETY
SIOC 1950
ROYAL SOCIETY OF CHEMISTRY
rsc.li/frontiers-organic

ORGANIC CHEMISTRY FRONTIERS

RESEARCH ARTICLE

View Article Online
View Journal | View Issue

Cite this: *Org. Chem. Front.*, 2024, **11**, 6036

Synthesis of annulated rosarins *via* iminium activation†

Duong D. Nguyen,[a] Jorge Labella, *[b] Marta Gómez-Gómez, [b] Tomás Torres *[b,c,d] and Jonathan L. Sessler *[a]

Applications of expanded porphyrins, pyrrole-based macrocycles known for their unique optoelectronic properties, have been hampered by challenges associated with their synthesis. Typically, these compounds are prepared *via* condensation–macrocyclization reactions under acidic conditions, using pyrrolic nucleophiles and aldehydes as electrophiles. The yield of these transformations is heavily influenced by the electrophilicity of the aldehydes, thus limiting the scope of the reaction. In this study, we demonstrate that activation of aldehydes by pre-conversion to the corresponding iminium species can be exploited for the construction of expanded porphyrins. Specifically, we employ iminium-based activation to prepare a series of naphthorosarins (NRos) using various aldehydes as electrophiles, resulting in different *meso* substituents. This approach has proved to be more efficient than classical methodologies, paving the way for the synthesis of previously inaccessible systems. Based on a combination UV-vis spectroscopy, electrochemistry, and density functional theory (DFT) and time-dependent DFT (TD-DFT) calculations, the *meso*-substituent affect slightly the optoelectronic properties of the NRos considered in this study. Theoretical calculations provide support for the conclusion that the iminium pathway makes the condensation reaction both kinetically and thermodynamically more favorable. The present approach may provide a general tool useful in the synthesis of expanded porphyrins and other pyrrolic macrocycles.

Received 24th August 2024,
Accepted 12th September 2024

DOI: 10.1039/d4qo01559b

rsc.li/frontiers-organic

Introduction

Expanded porphyrins, macrocycles featuring more than four pyrrolic or related aromatic subunits,[1,2] have garnered significant attention due to their versatile electronic states and ability to stabilize radical forms and various aromatic configurations, including Hückel, Möbius, and excited-state (anti-)aromaticity.[3–7] Despite considerable progress in their chemistry, the synthesis of most expanded porphyrins remains a substantial challenge. The most common approach involves condensing a nucleophilic pyrrole derivative with an aldehyde electrophile, activated by either Brønsted or Lewis acids, followed by oxidation.[8] Other methods involving oxidative couplings[9,10] or cross-coupling reactions,[11–13] have also been reported. The success of the condensation strategy is significantly influenced by the electrophilicity of the aldehyde; higher electrophilicity makes the key condensation reaction more favourable, thereby increasing the yield of the entire cyclization process. For this reason, fluorinated aldehydes are often employed, while less electrophilic aldehydes, on the contrary, frequently result in unacceptably poor yields or even failed macrocyclizations.[14] This limitation significantly restricts the choice of *meso*-substituents, which play a crucial role in modulating the photophysical properties and potential applications of porphyrinoids.[15–21] Therefore, there is an incentive to enhance the reactivity of the aldehyde. Doing so is expected to improve the synthesis of known expanded porphyrins and may allow the preparation of derivatives nominally derived from less-activated aldehydes.

Iminium catalysis has emerged in recent decades as a powerful tool for the activation of aldehydes under simple, mild reaction conditions.[22] This kind of catalysis has been exploited in many transformations, including Michael additions, Diels–Alder cycloadditions, Knoevenagel condensations, and, more recently, photochemical reactions. Remarkably, more than 15 years ago, the groups of Singh[23,24] and Benaglia[25] reported the iminium-catalysed synthesis of dipyrromethenes, key intermediates in the formation of expanded porphyrins. However, to our knowledge, the preparation of expanded porphyrins *via* iminium chemistry has never been reported.

[a]*Department of Chemistry, The University of Texas at Austin, 105 E 24th Street A5300, Austin, TX, 78712, USA. E-mail: sessler@cm.utexas.edu*
[b]*Departamento de Química Orgánica, Universidad Autónoma de Madrid, Campus de Cantoblanco, C/Francisco Tomás y Valiente 7, 28049 Madrid, Spain. E-mail: jorge.labella@uam.es, tomas.torres@uam.es*
[c]*Institute for Advanced Research in Chemical Sciences (IAdChem), Universidad Autónoma de Madrid, 28049 Madrid, Spain*
[d]*IMDEA-Nanociencia, Campus de Cantoblanco, 28049 Madrid, Spain*
†Electronic supplementary information (ESI) available. See DOI: https://doi.org/10.1039/d4qo01559b

Herein we report the synthesis of a representative class of expanded porphyrins, namely the naphthorosarins (NRos; Fig. 1), employing iminium-catalysed condensation conditions. As detailed below, we have found that the addition of secondary amines significantly enhances the macrocyclization yield, enabling the synthesis of NRos with various electron-donating *meso*-substituents. Density Functional Theory (DFT) calculations reveal that the origin of this enhancement lies in the higher concentration of "activated" aldehyde available to initiate the condensation and a reaction sequence that involves a more favourable rate-determining step. To provide a preliminary insight into the effect of *meso*-groups on the opto-electronic properties of the macrocycle, the present NRos were studied by a combination of UV-vis spectroscopic analyses and electrochemical measurements, as well as supporting DFT and time-dependent DFT (TD-DFT) calculations.

Results and discussion

Optimization, scope, and reaction mechanism of iminium-based macrocyclization

NRos are an intriguing class of expanded porphyrins characterized by an antiaromatic, planar π-skeleton.[26–30] The synthesis of these derivatives relies on the acid-catalysed condensation of naphthobipyrrole (**NBP**) with a suitable aldehyde,[31–33] followed by DDQ oxidation. The yield of this condensation is particularly dependent on the aldehyde reactivity. We thus considered NRos to be a near-ideal system with which to explore the iminium-catalysed synthesis of expanded porphyrins. Thus, **NRos 1**, featuring 2,6-dimethylphenyl groups as *meso*-substituents, was selected as a model substrate since 2,6-dimethylbenzaldehyde (a) did not show any reactivity under conditions effective for the preparation of **NRos** bearing electron-withdrawing substituents; even in such cases, the yields are often low (*e.g.*, 5–15%; *cf.* Scheme where the yields using the previous standard protocol are shown in parentheses). The same conditions were then tested but in the presence of 50% mol morpholine. Again, no detectable **NRos 1** was found in the reaction mixture. Adding 3 equiv. of trifluoroacetic acid (TFA) to promote the formation of a putative iminium intermediate, resulted in the formation of trace quantities of **NRos 1**. The addition of 6 equiv. further enhanced the macrocyclization process and allowed for the isolation of **NRos 1** in 3% yield. Other secondary amines, namely piperidine and pyrrolidine, were then tested. Using the latter secondary amine, allowed a yield of 8% to be achieved. The use of 6 equiv. of TFA in the absence of pyrrolidine did not result in the formation of **NRos 1**, providing support for the notion that the reaction takes place *via* an iminium intermediate. Consistent with this conclusion was the finding that *N*-methyl-pyrrolidine in the presence of TFA was ineffective as a catalyst. Specifically, no **NRos 1** was detected in the reaction medium under these conditions.

Using the above conditions, we next explored reactions between **NBP** and various aldehydes. For these studies, several highly electron-rich aldehydes, such as 4-(*tert*-butyl)benzaldehyde, 4-(dimethylamino)benzaldehyde and 3,5-dimethoxybenzaldehyde, were studied. While evidence of reactivity was observed the resulting compounds suffered from low solubility and stability, precluding their full characterization. In order to quantitatively evaluate the effect of iminium catalysis, we decided to employ aldehydes known to afford stable and soluble NRos under conventional conditions (Scheme 1). The goal was to see if these yields could be increased. For this

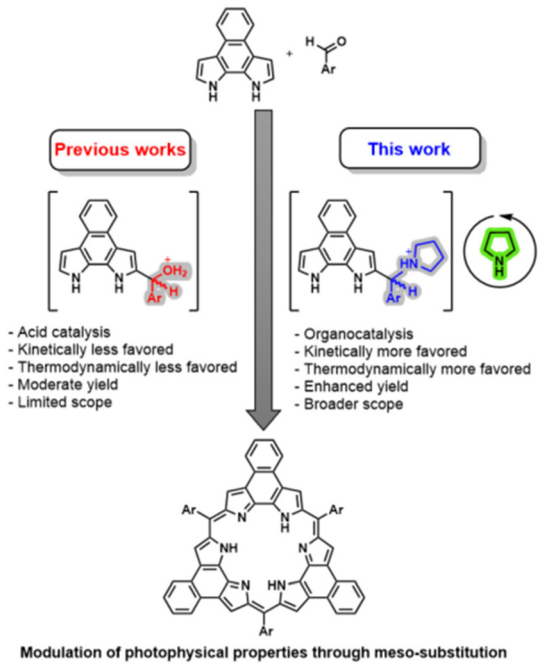

Fig. 1 New strategy for the synthesis of expanded porphyrins.

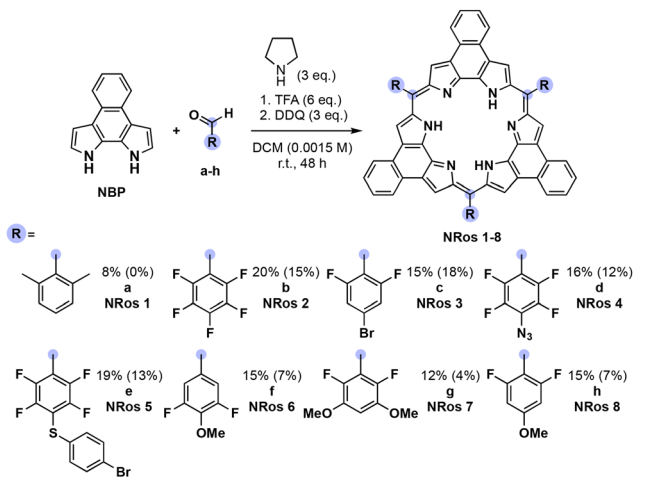

Scheme 1 Iminium-based macrocyclization reaction of **NBP** with various aldehydes. Reagents and conditions: (1) aldehydes (1.2 equiv.), pyrrolidine (3 equiv.), TFA (6 equiv.), DCM, 25 °C, 48 h. (2) 2,3-dichloro-5,6-dicyano-1,4-benzoquinone (DDQ) (3 equiv.), DCM, 25 °C, 2.5 h. Yields in the absence of catalyst are given in parentheses.

portion of the study, we selected several different aldehydes, including (i) **b**, since it is among the most common aldehydes employed for the synthesis of expanded porphyrins, (ii) **c**–**e** as they present functional groups capable of undergoing post-synthetic functionalization, and (iii) **f**–**h**, which bear methoxy groups at different positions. In all cases, the iminium-catalysed reaction led to higher yields, with increases of 33–200% being seen compared to the conventional method. The relative yield enhancement was greatest for aldehydes bearing fewer fluorine atoms, systems that give rise to the lowest macrocyclization yield using the conventional conditions. This highlights the positive effect of the present iminium-based approach.

To shed light on the influence of iminium generation on the macrocyclization process, the reaction pathway was quantitatively compared to the non-iminium pathway by means of DFT calculations (see ESI† for computational details). Fig. 2 shows the calculated free energy profiles considering **a** as the aldehyde (*i.e.*, **NRos 1** formation). Our model assumes that the reaction proceeds from an activated carbonyl species, derived from either classic protonation (path α) or iminium formation (path β) of the carbonyl moiety in **a** (**Reacα** and **β**, respectively). The formation of these species proved to be energetically favoured in path β (Boltzmann distribution: $F(a)/F(\textbf{Reac}\alpha) = 4.7 \times 10^{27}$ while $F(a)/F(\textbf{Reac}\beta) = 2.3 \times 10^{12}$). The first C–C bond-forming step of the reaction then involves nucleophilic attack of **NBP** on either **Reacα** and **β**. This step is kinetically more favourable in the former case, which is consistent with the higher stability of **Reac β**. This reaction, which leads to **IN1α/β**, seems to be highly reversible in the case of path β. The next step along the reaction coordination is a 1,3-H shift, an isomerization characterized by the highest activation energy in both pathways (37.3 kcal mol^{-1} and 30.3 kcal mol^{-1} for paths α and β, respectively). Crucially, this reaction step is kinetically and thermodynamically more favoured in the iminium-catalysed process. Indeed, the formation of **IN2** is endergonic in the case of path α, while it is exergonic in the case of path β. Finally, **IN3**, which is common to both pathways, undergoes an SN1-type reaction, giving rise to the corresponding dipyrromethene (**Prod**), which by sequential reactions with activated carbonyl species would afford the reduced form of **NRos 1**. Based on these results, we suggest that the enhanced reactivity observed when using secondary amines is essentially due to (i) a higher concentration of activated carbonyl (**Reacα/β**) available to start the condensation and (ii) the lower activation barrier and greater exergonicity of the rate-determining 1,3-H shift step.

Role of *meso*-groups on the opto-electronic properties of NRos

To assess the influence of *meso*-substituents on the optical properties of the macrocycle, UV-vis spectra of **NRos 2–8** were recorded in dichloromethane at a concentration of 5.0×10^{-6} (M). As depicted in Fig. 3, the absorption spectrum of **NRos 2–8** is primarily characterized by a broad band that covers the 350 to 700 nm spectral region. Although the absorption maxima show minimal variations (467–481 nm), a discernible influence of the *meso*-group is observed. Specifically, the absorption maxima of **NRos 6–8**, all of which possess relatively electron-donating *meso*-aryl substituents are all above 470 nm,

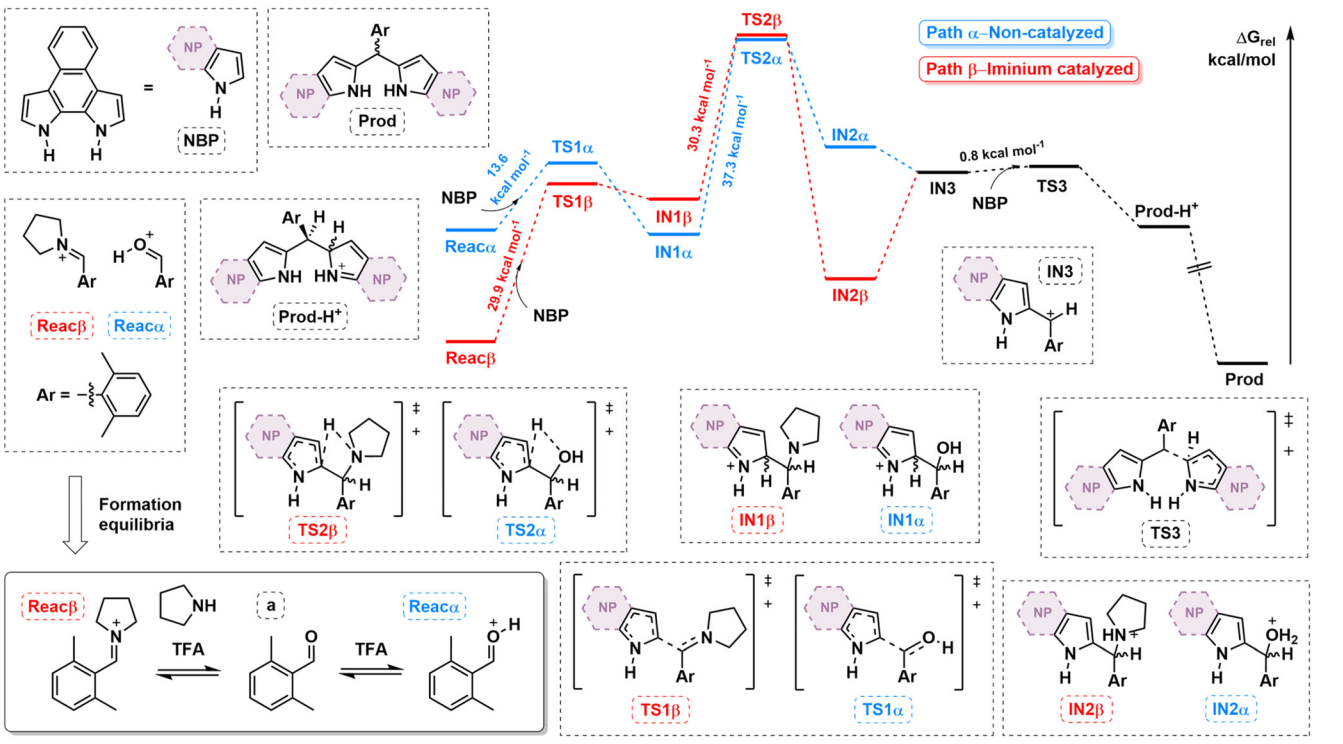

Fig. 2 Relative energy profile for the DFT reaction mechanism of the macrocyclization process calculated at the B3LYP/6-31G(d,p) level, considering aldehyde **a** as model substrate. The influence of the iminium generation (red) is compared to the non-iminium pathway (blue).

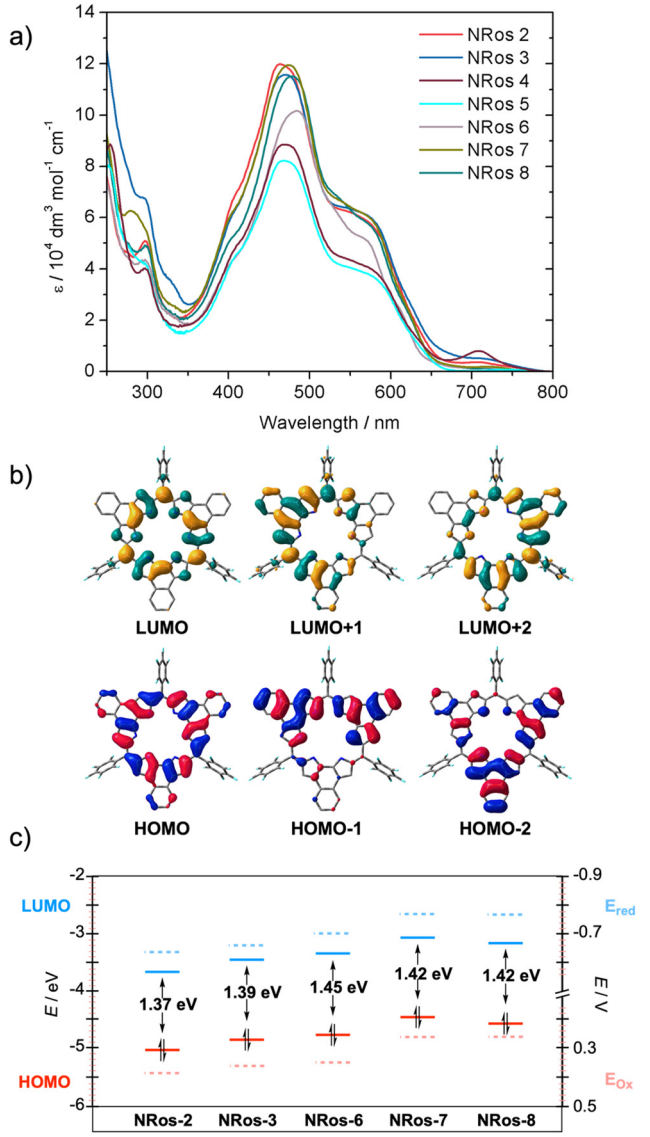

Fig. 3 Optical and electrochemical properties of **NRos 2–8** (a) UV-vis-NIR spectra in dichloromethane (5.0×10^{-6} M) at room temperature. (b) Selected molecular orbitals of **NRos-2**, which serves as example, calculated by DFT at the CAM-B3LYP/6-31G(d,p) level of theory. Isosurface value = 0.02. Hydrogen atoms are omitted for clarity. (c) Calculated HOMO–LUMO energies (solid) and electrochemical oxidation and reduction potentials obtained by cyclic voltammetry in CH_2Cl_2 (dashed lines) of **NRos 2**, **3**, **6**, **7** and **8**.

while the more electron-deficient **NRos 2–5** display maxima below this value. As revealed by time-dependent density functional calculations (TD-DFT), the broad absorption seen for the **NRos** arises mainly from HOMO → LUMO+1 and HOMO → LUMO+2 transitions, corresponding to S0 → S5 and S0 → S6 excitations. Note: selected TD-DFT transition energies, oscillator strengths (f), and molecular orbital configurations are shown in Tables S7.1–7.5.† As illustrated in Fig. 3b, the methine bridge is minimally involved in these orbitals, explaining the slight effect of the *meso*-groups on the absorption maxima. In all cases, the absorption profiles exhibit a similar shape, suggesting that the *meso*-groups do not significantly perturb the electronic distribution of the macrocycle. Regarding the emission properties, these NRoss displayed no appreciable fluorescence, which is consistent with previous results.[26]

The effect of *meso*-groups on the oxidation/reduction potential was evaluated using cyclic and differential pulse voltammetry (see Fig. 3c and S6.1†) in CH_2Cl_2. To ensure a reliable comparison, we mainly focused on soluble **NRos 2**, **3**, **6**, **7** and **8**. Fig. 3c shows the potentials for the first oxidation/reduction processes (see ESI† for second oxidation/reduction potentials and more details) and the calculated HOMO–LUMO levels thought to govern these redox processes. A strong correlation between the observed redox potential and the calculated HOMO–LUMO gap was observed. As expected, **NRos 2** exhibits the deepest LUMO level and accordingly the lowest reduction potential. A clear influence of the group at the *para*-position of the *meso*-aryl is noticeable when comparing **NRos 3** and **NRos 8**. Thus, a bromine atom makes *meso*-aryls less electron-rich compared to methoxy group, leading to higher oxidation and reduction potential. On the other hand, **NRos 6** is easier to reduce than **NRos 8**, despite fluorine atoms that are farther from the *meso*-carbon. We hypothesize that this difference arises from the possible planarization of the electron-deficient *meso*-aryl in **NRos 6**, thus enabling better conjugation. On the other hand, the introduction of two methoxy groups (**NRos 7**) lowers the reduction/oxidation potentials. It should be noted that although the position of HOMO–LUMO levels in all these species varies slightly, the bandgap of the NRos is rather similar, consistent with the UV-vis absorption experiments.

Conclusions

In summary, we have shown that the generation of iminium species is a promising approach to increase the yield and broaden the preparative scope in the case of a test expanded porphyrin, naphthorosarin (**NRos**). Specifically, the presence of secondary amines, in conjunction with an acid catalyst, significantly improves the macrocyclization yield and provides access to previously inaccessible **NRos**. DFT calculations provide support for the suggestion that iminium generation lowers the activation energy of key steps during macrocyclization, including rate-determining proton transfers, while stabilizing most intermediates. This method has enabled the preparation of multiple **NRos**, which differ in their *meso*-substituents. The nature of the *meso*-groups, in turn, was found to affect slightly key properties of the products, such as the absorption maximum and the HOMO–LUMO levels.

Ultimately, the iminium-based method described here is expected to provide a new tool that can be exploited for the synthesis and thus study of expanded porphyrins.

Data availability

The data supporting the findings of this study are available within the article and its ESI.†

Conflicts of interest

There are no conflicts to declare.

Acknowledgements

The work in Austin was supported by the Robert A. Welch Foundation (F-0018 to J. L. S.) and by the National Science Foundation (CHE-2304731) subsequent to Nov. 1, 2023. T. T. acknowledges financial support from the Spanish MCIN/AEI/10.13039/501100011033 and European Union NextGenerationEU/PRTR (PID2020-116490GB-I00, TED2021-131255B-C43), MCIU/AEI/10.13039/501100011033/FEDER, UE (PID2023-151167NB-I00), the Comunidad de Madrid and the Spanish State through the Recovery, Transformation and Resilience Plan ["Materiales Disruptivos Bidimensionales (2D)" (MAD2D-CM) (UAM1)-MRR Materiales Avanzados], and the European Union through the Next Generation EU funds. IMDEA Nanociencia acknowledges support from the "Severo Ochoa" Programme for Centres of Excellence in R&D (MINECO, Grant SEV2016-0686). T. T. also acknowledges the Alexander von Humboldt Foundation (Germany) for the A. v. Humboldt – J. C. Mutis Research Award 2023 (Ref 3.3 - 1231125 - ESP-GSA). M. G-G. acknowledges MECD, Spain, for a F.P.U. fellowship. We acknowledge the generous allocation of computer time at the Centro de Computación Científica at the Universidad Autónoma de Madrid (CCC-UAM).

References

1 (*a*) V. V. Roznyatovskiy, C. Lee and J. L. Sessler, π-Extended isomeric and expanded porphyrins, *Chem. Soc. Rev.*, 2013, **42**, 1921–1933; (*b*) S. Saito and A. Osuka, Expanded Porphyrins: Intriguing Structures, Electronic Properties, and Reactivities, *Angew. Chem., Int. Ed.*, 2011, **50**, 4342–4373.

2 (*a*) T. K. Chandrashekar and S. Venkatraman, Core-Modified Expanded Porphyrins: New Generation Organic Materials, *Acc. Chem. Res.*, 2003, **36**, 676–691; (*b*) R. Misra and T. K. Chandrashekar, Structural Diversity in Expanded Porphyrins, *Acc. Chem. Res.*, 2008, **41**, 265–279.

3 J. Kim, J. Oh, A. Osuka and D. Kim, Porphyrinoids, a unique platform for exploring excited-state aromaticity, *Chem. Soc. Rev.*, 2022, **51**, 268–292.

4 M. Stępień, L. Latos-Grażyński, N. Sprutta, P. Chwalisz and L. Szterenberg, Expanded Porphyrin with a Split Personality: A Hückel–Möbius Aromaticity Switch, *Angew. Chem., Int. Ed.*, 2007, **46**, 7869–7873.

5 Z. S. Yoon, A. Osuka and D. Kim, Möbius aromaticity and antiaromaticity in expanded porphyrins, *Nat. Chem.*, 2009, **1**, 113–122.

6 G. I. Vargas-Zúñiga and J. L. Sessler, *Advances in Inorganic Chemistry*, ed. R. van Eldik and R. Puchta. 2018. pp. 327–377.

7 A. Alka, V. S. Shetti and M. Ravikanth, Coordination chemistry of expanded porphyrins, *Coord. Chem. Rev.*, 2019, **401**, 213063.

8 T. Tanaka and A. Osuka, Chemistry of *meso*-Aryl-Substituted Expanded Porphyrins: Aromaticity and Molecular Twist, *Chem. Rev.*, 2017, **117**, 2584–2640.

9 D. Seidel, V. Lynch and J. L. Sessler, Cyclo[8]pyrrole: A Simple-to-Make Expanded Porphyrin with No Meso Bridges, *Angew. Chem., Int. Ed.*, 2002, **41**, 1422–1425.

10 M. Takase, V. Enkelmann, D. Sebastiani, M. Baumgarten and K. Müllen, Annularly Fused Hexapyrrolohexaazacoronenes: An Extended π System with Multiple Interior Nitrogen Atoms Displays Stable Oxidation States, *Angew. Chem., Int. Ed.*, 2007, **46**, 5524–5527.

11 M. W. Harry, A. Bhaskar, G. Ramakrishna, T. Goodson III, M. Imamura, A. Mawatari, K. Nakao, H. Enozawa, T. Nishinaga and M. Iyoda, Giant Thienylene-Acetylene-Ethylene Macrocycles with Large Two-Photon Absorption Cross Section and Semishape-Persistence, *J. Am. Chem. Soc.*, 2008, **130**, 3252–3253.

12 J. Krömer, I. Rios-Carreras, G. Fuhrmann, C. Musch, M. Wunderlin, T. Debaerdemaeker, E. Mena-Osteritz and P. Bäuerle, Synthesis of the First Fully α-Conjugated Macrocyclic Oligothiophenes: Cyclo[*n*]thiophenes with Tunable Cavities in the Nanometer Regime, *Angew. Chem., Int. Ed.*, 2000, **39**, 3481–3486.

13 G. Fuhrmann, T. Debaerdemaeker and P. Bäuerle, C–C bond formation through oxidatively induced elimination of platinum complexes—A novel approach towards conjugated macrocycles, *Chem. Commun.*, 2003, 948–949.

14 J. S. Lindsey, Synthetic Routes to *meso*-Patterned Porphyrins, *Acc. Chem. Res.*, 2010, **43**(2), 300–311.

15 H. Hata, H. Shinokubo and A. Osuka, Anthracene-Bridged Z-Shaped [26]Hexaphyrin(1.1.1.1.1.1) Dimer from the Regioselective Diels–Alder Reaction of a Hexaphyrin with Bis-*o*-xylylene Equivalents, *Angew. Chem., Int. Ed.*, 2005, **44**, 932–935.

16 J.-Y. Shin, T. Tanaka, A. Osuka, Q. Miao and D. Dolphin, BODIPY–Hexaphyrin Hybrids, *Chem. – Eur. J.*, 2009, **15**, 12955–12959.

17 A. Werner, M. Michels, L. Zander, J. Lex and E. Vogel, "Figure Eight" Cyclooctapyrroles: Enantiomeric Separation and Determination of the Absolute Configuration of a Binuclear Metal Complex, *Angew. Chem., Int. Ed.*, 1999, **38**, 3650–3653.

18 A. K. Burrell, G. Hemmi, V. Lynch and J. L. Sessler, Uranylpentaphyrin: an actinide complex of an expanded porphyrin, *J. Am. Chem. Soc.*, 1991, **113**, 4690–4692.

19 J. L. Sessler, D. Seidel, A. E. Vivian, V. Lynch, B. L. Scott and D. W. Keogh, Hexaphyrin(1.0.1.0.0.0): An Expanded

Porphyrin Ligand for the Actinide Cations Uranyl (UO_2^{2+}) and Neptunyl (NpO_2^{+}), *Angew. Chem., Int. Ed.*, 2001, **40**, 591–594.

20 X. J. Zhu, S. T. Fu, W. K. Wong, J. P. Guo and W. Y. Wong, A Near-Infrared-Fluorescent Chemodosimeter for Mercuric Ion Based on an Expanded Porphyrin, *Angew. Chem., Int. Ed.*, 2006, **45**, 3150–3154.

21 D. Wu, A. B. Descalzo, F. Weik, F. Emmerling, Z. Shen, X. Z. You and K. A. Rurack, A Core-Modified Rubyrin with *meso*-Aryl Substituents and Phenanthrene-Fused Pyrrole Rings: A Highly Conjugated Near-Infrared Dye and Hg^{2+} Probe, *Angew. Chem., Int. Ed.*, 2008, **47**, 193–197.

22 A. Erkkila, I. Majander and P. M. Pihko, Iminium Catalysis, *Chem. Rev.*, 2007, **107**, 5416–5470.

23 K. Singh, S. Behal and M. S. Hundal, Efficient and versatile single pot approach to dipyrromethanes and bis(heterocyclyl)methanes, *Tetrahedron*, 2005, **61**, 6614–6622.

24 K. Singh, S. Behal and P. K. Deb, Efficient and Versatile Single–Pot Alternative Approach to Dipyrromethanes, *Synth. Commun.*, 2005, **35**, 929–934.

25 C. Biaggi, M. Benaglia, L. Raimondi and F. Cozzi, Organocatalytic synthesis of dipyrromethanes by the addition of *N*-methylpyrrole to aldehydes, *Tetrahedron*, 2006, **62**, 12375–12379.

26 M. Ishida, S. J. Kim, C. Preihs, K. Ohkubo, J. M. Lim, B. S. Lee, J. S. Park, V. M. Lynch, V. V. Roznyatovskiy, T. Sarma, P. K. Panda, C. H. Lee, S. Fukuzumi, D. Kim and J. L. Sessler, Protonation-coupled redox reactions in planar antiaromatic *meso*-pentafluorophenyl-substituted *o*-phenylene-bridged annulated rosarins, *Nat. Chem.*, 2013, **5**, 15–20.

27 S. Samala, R. Dutta, Q. He, Y. Park, B. Chandra, V. M. Lynch, Y. M. Jung, J. Sessler and C. Lee, A robust bis-rhodium(I) complex of π-extended planar, anti-aromatic hexaphyrin[1.0.1.0.1.0], *Chem. Commun.*, 2020, **56**, 758–761.

28 S. Fukuzumi, K. Ohkubo, M. Ishida, C. Preihs, B. Chen, W. T. Borden, D. Kim and J. L. Sessler, Formation of Ground State Triplet Diradicals from Annulated Rosarin Derivatives by Triprotonation, *J. Am. Chem. Soc.*, 2015, **137**, 9780–9783.

29 G. Kim, R. Dutta, W. Y. Cha, S. J. Hong, J. Oh, D. Firmansyah, H. Jo, K. M. Ok, C. H. Lee and D. Kim, Noncovalent Intermolecular Interaction in Cofacially Stacked 24π Antiaromatic Hexaphyrin Dimer, *Chem. – Eur. J.*, 2020, **26**, 16434–16440.

30 J. Chen, A. C. Sedgwick, S. Sen, Y. Ren, Q. Sun, C. Chau, J. F. Arambula, T. Sarma, L. Song, J. L. Sessler and C. Liu, Expanded porphyrins: functional photoacoustic imaging agents that operate in the NIR-II region, *Chem. Sci.*, 2021, **12**, 9916–9921.

31 D. D. Nguyen, J. Labella, J. Laforga-Martin, C. L. Folcia, J. Ortega, T. Torres, T. Sierra and J. L. Sessler, Columnar liquid crystals based on antiaromatic expanded porphyrins, *Chem. Commun.*, 2024, **60**, 3401–3404.

32 D. Firmansyah, S. J. Hong, R. Dutta, Q. He, J. Bae, H. Jo, H. Kim, K. M. Ok, V. M. Lynch, H. R. Byon, J. L. Sessler and C. H. Lee, Trapping of Stable [4*n*+1] π-Electron Species from Peripherally Substituted, Conformationally Rigid, Antiaromatic Hexaphyrins, *Chem. – Eur. J.*, 2019, **25**, 3525–3531.

33 S. Lee, Y. Wang, R. Dutta, C. H. Lee, J. L. Sessler and D. Kim, Xanthene-Separated 24 π-Electron Antiaromatic Rosarin Dimer, *Chem. – Eur. J.*, 2023, **29**, e202301501.